THE JOURNAL OF
PHYSICAL CHEMISTRY
Letters

pubs.acs.org/JPCL Letter

Superconducting Zirconium Polyhydrides at Moderate Pressures

Hui Xie,[#] Wenting Zhang,[#] Defang Duan,* Xiaoli Huang,* Yanping Huang, Hao Song, Xiaolei Feng, Yansun Yao, Chris J. Pickard, and Tian Cui*

Cite This: *J. Phys. Chem. Lett.* 2020, 11, 646−651

Read Online

ACCESS | Metrics & More | Article Recommendations | SI Supporting Information

ABSTRACT: Highly compressed hydrides have been at the forefront of the search for high-T_c superconductivity. The recent discovery of record-high T_c's in H_3S and $LaH_{10\pm x}$ under high pressure fuels the enthusiasm for finding good superconductors in similar hydride groups. Guided by first-principles structure prediction, we successfully synthesized ZrH_3 and Zr_4H_{15} at modest pressures (30−50 GPa) in diamond anvil cells by two different reaction routes: ZrH_2 + H_2 at room temperature and Zr + H_2 at ∼1500 K by laser heating. From the synchrotron X-ray diffraction patterns, ZrH_3 is found to have a $Pm\bar{3}n$ structure corresponding to the familiar A15 structure, and Zr_4H_{15} has an $I\bar{4}3d$ structure isostructural to Th_4H_{15}. Electrical resistance measurement and the dependence of T_c on the applied magnetic field of the sample showed the emergence of two superconducting transitions at 6.4 and 4.0 K at 40 GPa, which correspond to the two T_c's for ZrH_3 and Zr_4H_{15}.

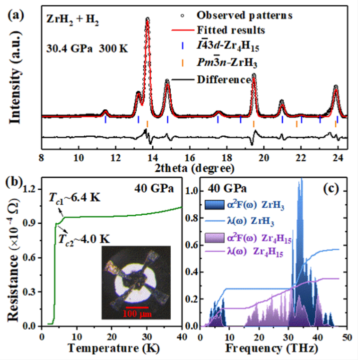

Theoretical studies suggest that highly compressed hydrogen-rich materials hold promise as high-temperature (T_c) superconductors.[1−3] The recent discovery of superconductivity above 203 K and 250−260 K in compressed H_3S[4,5] and $LaH_{10\pm x}$[6,7] marks a milestone in superconductivity research. This discovery is groundbreaking, not only for representing the highest T_c's ever observed in all materials since the discovery of superconductivity but also for being the first time that previously unknown high-T_c superconductors were predicted by theory[8−10] and afterward verified by experiment. Even before H_3S and $LaH_{10\pm x}$, theoretical prediction has had notable success in searching for superconducting polyhydrides. SiH_4 and AlH_3 were first considered because of their high hydrogen content among naturally existing hydrides.[11−14] Experiments revealed that compressed SiH_4 is superconducting with maximum T_c of 17.5 K at 96 GPa.[13] The experimental study confirmed the predicted structure of AlH_3 but could not detect the superconductivity down to 4 K.[14] It was then understood that the superconductivity in AlH_3 is suppressed by strong anharmonicity.[15] In recent years, the search for high-T_c hydrides has expanded substantially, from group IV to other main group hydrides,[16,17] and to transition metal hydrides. Many new polyhydrides have been predicted theoretically,[18−21] and some have already made their real-world appearance, including bulk RhH_2,[22] CoH_2,[23] FeH_5,[24] nanocrystal RhH,[25] etc.

Zirconium hydrides have been studied primarily for applications in hydrogen storage and nuclear technology, but not so much as potential superconductors. For example, zirconium and its alloys are widely used as protective casings for nuclear reactor cores.[26] In this case, zirconium alloy operates at high temperature and forms hydride upon combination with hydrogen produced by nuclear reactions. However, we expect to find good superconducting materials in Zr−H hydrides because of the rich structure diversity in this group. The stunning success in $LaH_{10\pm x}$ also fuels the enthusiasm for finding high T_c in similar hydride groups. Experimentally, stable ZrH and ZrH_2 and metastable δ-$ZrH_{1.5}$ have been successfully synthesized at ambient pressure, while ZrH_2 is the limit for hydrogen storage.[27,28] New stoichiometric ZrH_n ($n > 2$) hydrides with higher hydrogen concentration have been explored theoretically. First-principles studies up to 400 GPa suggest ZrH_3 is stable at ambient pressure and ZrH_4 and ZrH_6 are stable above 100 GPa.[29,30] These hydrides are calculated to be superconducting under high pressure,[30] which encourages the experimental realization.

Before conducting the experiment, we performed variable-composition searches for stable Zr−H compounds at 1 atm and 50 and 100 GPa using the CALYPSO[31] and AIRSS codes.[32] We compared our findings with previous calculations[29] and found a new stable compound Zr_4H_{15} (see Figure S1). The formation enthalpies (ΔH) of predicted Zr−H hydrides with zero-point energy (ZPE) were calculated with respect to the two sets of starting materials, Zr + H_2 (Figure 1a) and ZrH_2 + H_2 (Figure S2) at different pressures, from which global stability tie lines (convex hull) are constructed. Calculated ΔH shows that at ambient pressure ZrH ($P4_2/mmc$) and ZrH_2 ($I4/mmm$) are the only two stable

Received: December 8, 2019
Accepted: January 4, 2020
Published: January 4, 2020

https://dx.doi.org/10.1021/acs.jpclett.9b03632

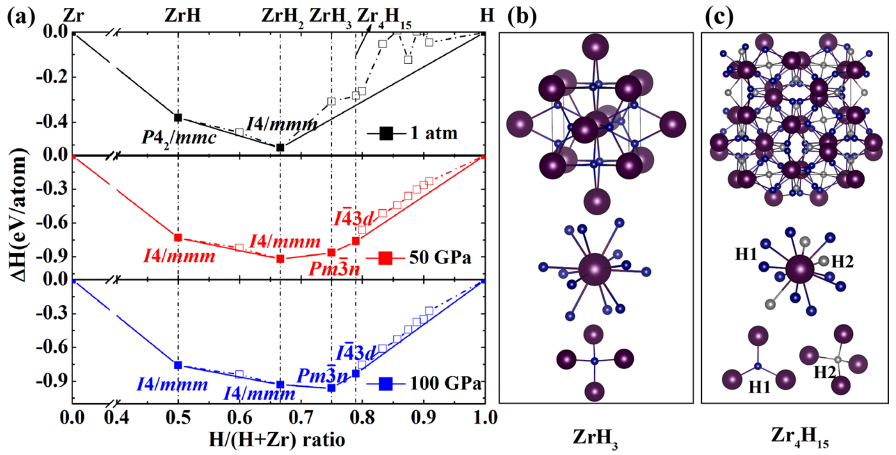

Figure 1. (a) Calculated formation enthalpies of zirconium hydrides with respect to decomposition into Zr and H_2 under pressure, including zero-point energies. Open symbols represent unstable configurations with respect to mixing lines on the convex hull, while solid symbols on the convex hull represent stable configurations. (b) Crystal structure of $Pm\bar{3}n$-ZrH_3. (c) Conventional unit cell of $I\bar{4}3d$-Zr_4H_{15}.

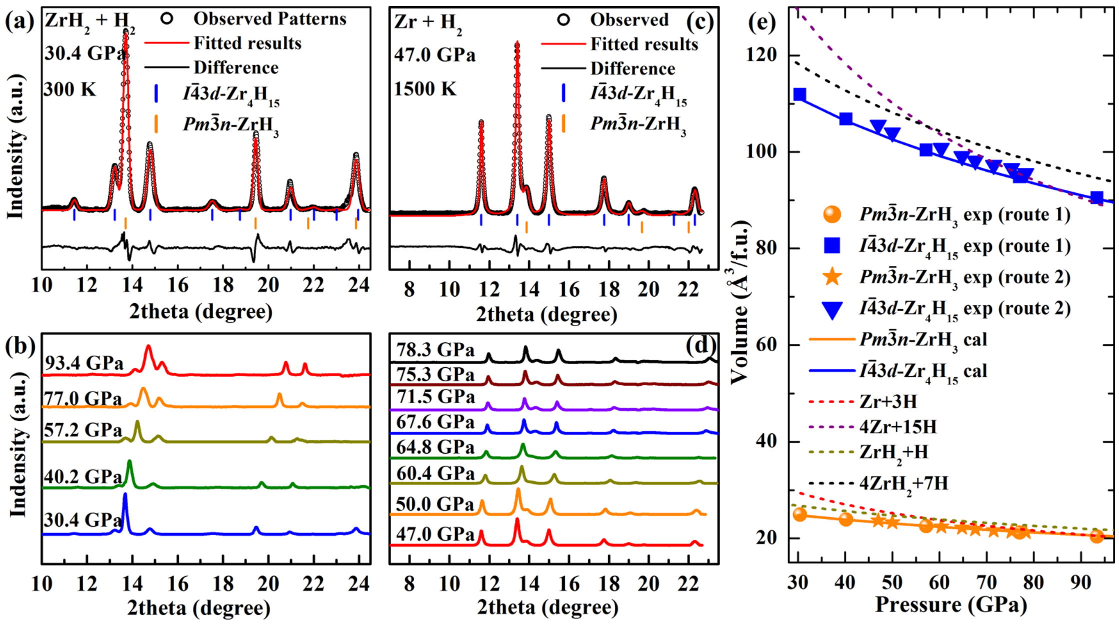

Figure 2. (a) Le Bail refinement plot of powder XRD data ($\lambda = 0.6199$ Å) obtained in $ZrH_2 + H_2$ reaction route at 30.4 GPa. Open circles, experimental data; red curve, model fit for the structures; blue and orange ticks, Bragg diffraction positions for $I\bar{4}3d$-Zr_4H_{15} and $Pm\bar{3}n$-ZrH_3; black curve, residues. The reliability factors are $R_p = 9.05\%$ and $R_{wp} = 18.38\%$. (b) Evolution of the XRD pattern of panel a with increasing pressure. (c) Refinement of the experimental XRD patterns obtained in Zr + H_2 reaction route at 47.0 GPa. Reliability parameters are as $R_p = 7.44\%$ and $R_{wp} = 12.68\%$. (d) Evolution of the XRD pattern of panel c with increasing pressure. (e) Experimentally obtained volume per formula unit for ZrH_3 and Zr_4H_{15} in comparison to theoretical calculations as a function of pressure. Volumes for ideal mixtures of ZrH_2 + H, $4ZrH_2$ + 7H, Zr + 3H, and 4Zr + 15H are also plotted.

stoichiometries, in agreement with experimental results.[27,28] At 50 GPa, $Pm\bar{3}n$-ZrH_3 and $I\bar{4}3d$-Zr_4H_{15} enter the convex hull, indicating that they are likely synthesizable at this pressure. Meanwhile, the stable structure of ZrH changes to $I4/mmm$. At 100 GPa, the available stoichiometries stay the same, but ZrH_3 becomes the most stable stoichiometry. In this pressure range, all hydrides with the H/Zr ratio greater than 15:4 are metastable. All obtained stable structures were examined by phonon calculations, which show no imaginary modes and therefore establish their dynamic stability (see Figure S3). ZrH_3 has A15 structure with $Pm\bar{3}n$ symmetry (Figure 1b), in agreement with previous theoretical predictions.[29,30] Zr_4H_{15} has a cubic structure with $I\bar{4}3d$ symmetry (Figure 1c), which is isostructural to Th_4H_{15}.[33] In this structure, Zr atoms occupy the 16*c* sites, while H atoms occupy 48*e* (H1 in blue) and 12*a* (H2 in gray) sites. As shown in Figure 1c, each Zr atom is bonded to 12 H atoms, among which 3 are at 12*a* and 9 are at 48*e*. The H atoms at 48*e* and 12*a* are bonded to 3 and 4 Zr atoms, respectively. To the best of our knowledge, this is the first time such structures have been found in group IVB hydrides.

With the predicted structures at hand, we performed the synthesis via two reaction routes. The first was to react ZrH_2 with H_2 at room temperature in the DAC. After the target sample was loaded into DAC, the sealed pressure was maintained at around 30.4 GPa. Figure 2a shows the XRD pattern collected at 30.4 GPa, in which all Bragg peaks can be indexed to either the $Pm\bar{3}n$-ZrH_3 or $I\bar{4}3d$ -Zr_4H_{15} structure.

Table 1. Calculated Superconducting Transition Temperatures (T_c, K), EPC Constant (λ), Logarithmic Average Phonon Frequency (ω_{log}, K), Electronic DOS at the Fermi Level ($N(\varepsilon_f)$, states/eV/f.u.), Average of Squared Phonon Frequency ($\langle\omega^2\rangle$, THz^2), and Average Electron−Phonon Matrix Element ($\langle I^2\rangle$, eV^3/states)[a]

hydride (pressure)	T_c (K) (μ^* = 0.1−0.13)	λ	ω_{log}	$N(\varepsilon_f)$	$\langle\omega^2\rangle$	$\langle I^2\rangle$
Zr_4H_{15} (40 GPa)	0.2−0.8	0.33	792	3.55		
ZrH_3 (10 GPa)	12.5−16.6	0.68	518	0.88		
ZrH_3 (20 GPa)	9.8−13.8	0.61	571	0.85		
ZrH_3 (40 GPa)	8.4−12.4	0.57 (51%)	646	0.81 (10%)	650.6	0.74
H_3S (200 GPa)	211.6−230.2	1.88 (>80%)	1266	0.62 (43%)	962.2	1.81

[a] Percentages in parentheses represent the contribution of H atoms to the total λ and $N(\varepsilon_f)$.

The occurrence of a physical mixture of ZrH_3 and Zr_4H_{15} at this pressure is consistent to the energetic analysis (Figure 1a). A Le Bail refinement of the diffraction pattern recorded at 30.4 GPa yielded the lattice parameters for the two cubic unit cells, e.g., a = 3.676 Å for ZrH_3 and a = 7.636 Å for Zr_4H_{15}. During pressurization to 93.4 GPa (Figure 2 b), the diffraction peaks shift toward higher angles because of the reduction of lattice spacing but the overall pattern remains largely unchanged, indicating no other phases present in this pressure range. The second approach was to react Zr directly with H_2 in a laser-heated DAC. Initially, Zr and H_2 samples were loaded into the sample chamber of the DAC at lab conditions. The sample was then compressed to 47.0 GPa and laser-heated to 1500 K, from which the in situ synchrotron XRD pattern was measured. As shown in Figure 2c, the refined results show that all the observed peaks can be well indexed to $Pm\bar{3}n$-ZrH_3 and $I\bar{4}3d$-Zr_4H_{15} structures. Thus, the reaction products are the same as in the first reaction pathway, but the ratio of the two components seems different, as seen from the relative changes in the peak intensities. Upon further compression up to 78.3 GPa, no further transformation to any other phases was observed (Figure 2d).

Experimentally obtained volumes per formula unit (f.u.) for ZrH_3 and Zr_4H_{15}, in comparison to the calculated values as functions of pressure, are plotted in Figure 2e. Clearly, the experimental equation of state (EOS) for both ZrH_3 and Zr_4H_{15} is in very good agreement with theory. To ascertain the identified high-pressure phases, we compare the EOSs of the two compounds to the volumes of physical mixtures representative of decomposition products at the same pressure.[34,35] As seen in Figure 2e, all physical mixtures have larger volumes than the ZrH_3 and Zr_4H_{15} compounds in the pressure range of interest, suggesting that the formation of these two compounds is thermodynamically allowed. The P−V data fitted with a third-order Birch−Murnaghan (BM) equation of state[36] give V_0 = 31.0 (5) Å^3, B_0 = 97 (7) GPa, and B_0' = 4 (fixed) for ZrH_3 and V_0 = 140 (3) Å^3, B_0 = 92 (9) GPa, and B_0' = 4 (fixed) for Zr_4H_{15}. The synthesis of ZrH_3 and Zr_4H_{15} represents the debut of the first group IVB hydrides with the hydrogen-to-metal ratio greater than 2.[27,37−39] Zirconium is in the same group in the periodic table as rhodium but has a smaller mass than the latter. As a result, ZrH_3 and Zr_4H_{15} have higher gravimetric hydrogen contents of 3.2 and 4.0 wt %, respectively, as compared to 1.9 wt % for RhH_2.[22] Extrapolation from the fitted unit cell volumes for ZrH_3 and Zr_4H_{15} at ambient pressure gives two high volumetric hydrogen densities of 166.6 and 180.8 g/L, greater than that of RhH_2 (163.7 g/L). Therefore, ZrH_3 and Zr_4H_{15} may have the potential for hydrogen storage applications if they are recoverable to ambient conditions.

Calculated band structures and projected density of states (PDOS) of ZrH_3 and Zr_4H_{15} at 40 GPa (Figure S6) show that both compounds are metallic with significant contributions of the Zr-d states to the DOS at the Fermi level. To investigate the phonon-mediated superconductivity, the EPC strength (λ) and logarithmic average frequency (ω_{log}) are calculated. The T_c is then estimated using the Allen−Dynes modified McMillan equation[40] with a Coulomb pseudopotential μ^*

$$T_c = \frac{\omega_{log}}{1.2}\exp\left[-\frac{1.04(1+\lambda)}{\lambda-\mu^*(1+0.62\lambda)}\right] \quad (1)$$

The calculated λ for Zr_4H_{15} is 0.33 at 40 GPa, and the ω_{log} is 792 K. Using a nominal value 0.13 for μ^*, the estimated T_c at 40 GPa is 0.2 K (see Table 1). Likewise, the calculated λ for ZrH_3 are 0.68, 0.61, and 0.57 at 10, 20, and 40 GPa, and the ω_{log} are 518, 571, and 646 K, respectively. Using μ^* = 0.13, the estimated T_c for ZrH_3 at 10, 20, and 40 GPa are 12.5, 9.8, and 8.4 K, respectively. ZrH_3 is therefore predicted to have a higher T_c than Zr_4H_{15}. To elucidate the mechanism, phonon dispersion curves and density of states (PHDOS), Eliashberg spectral function $\alpha^2F(\omega)$, and EPC integral $\lambda(\omega)$ are calculated for ZrH_3 at 40 GPa (Figure. 3). For the calculated λ of 0.57, the high-frequency H vibrational modes contribute about 51%. To identify the contributions of various phonon modes along different vibrational directions, solid circles with the radius proportional to the EPC strength are plotted on the phonon dispersion curves. Interestingly, the projected EPC along different directions are almost equal.

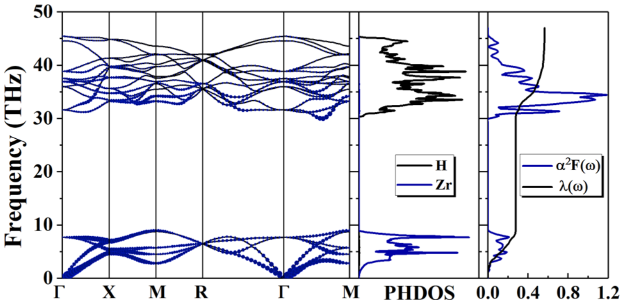

Figure 3. Phonon band structure, density of states, Eliashberg spectral function $\alpha^2F(\omega)$ and the EPC integral $\lambda(\omega)$ of ZrH_3 at 40 GPa. Size of the circle on the phonon band structure correspond to the contribution to the EPC.

To investigate the predicted superconductivity in ZrH_3 and Zr_4H_{15}, we carried out high-pressure variable-temperature electrical resistance measurements. To make the sample, we used NH_3BH_3 as the hydrogen source. The sample containing ZrH_2 and NH_3BH_3 was initially compressed to 30 GPa in the DAC and then laser-heated to 1600 K. After the reaction, the

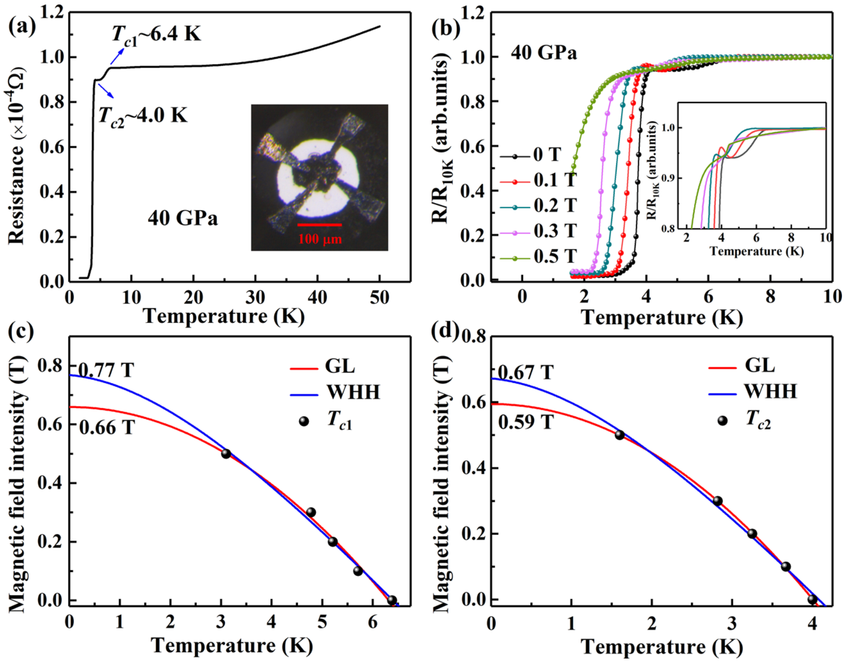

Figure 4. (a) Electrical resistance $R(T)$ curve of Zr−H sample at 40 GPa. Inset shows the photo of the sample after laser heating. (b) Superconducting transition of the sample with different applied magnetic field at 40 GPa. (c and d) Dependence of T_{c1} and T_{c2} on the external magnetic field H_c. The solid lines in blue and red represent fittings by WHH and GL equations, respectively.

sample was compressed to 40 GPa, at which two superconducting transitions were detected with pronounced zero resistance (Figure 4a). We proposed that these correspond to two T_c's for the two phases, one at 6.4 K (T_{c1}) and the other at 4.0 K (T_{c2}). We first ruled out the possibility that these two superconducting transitions belong to BN, NH_3BH_3, or ZrH_2 (Figure S6). From the XRD pattern of the prepared sample deposited with four electrodes, the sample contains both ZrH_3 and Zr_4H_{15} (Figure S7). On the basis of our calculation (Table 1), we tentatively interpret that the higher T_c is likely to be that of ZrH_3, and the lower one is for Zr_4H_{15}. The superconducting resistance drop $R(T)$ is also dependent on the applied magnetic field, further proving these two superconducting transitions. As demonstrated in Figure 4b, the two superconducting transition temperatures T_{c1} and T_{c2} shift to lower temperatures upon increasing the magnetic field (H_c) to 0.5 T. To determine the upper critical magnetic field $H_c(0)$, the extrapolation methods combined with the Ginzburg−Landau (GL) equation[41] and Werthdamer−Helfand−Hohenberg (WHH) equation[42] are shown in panels c and d of Figure 4, respectively.

It is generally accepted that anharmonicity can have noticeable influence on phonon-mediated superconductivity,[15,43] especially in structures with softened phonon modes. For example, in $Pm\bar{3}n$-AlH_3, anharmonicity can suppress the EPC and reduces the T_c from 24 to 2 K, giving the explanation for the discrepancy between experimental and theoretical results.[15] Although ZrH_3 has the same structure as AlH_3, its flat phonon spectrum implies that anharmonic effects on EPC are small. For ZrH_3, the experimentally determined T_c of 6.4 K is slight lower than the theoretical value of ~8.4 K. A possible reason for this discrepancy is that the actual Coulomb pseudopotential μ^* in ZrH_3 is greater than 1.3, approximately equal to 1.5. As pointed out previously,[44] the effects of Coulomb repulsion can be very large in low-density metals and it would be substantially underestimated if the nominal value is used in the McMillan equation, and this may be the case for zirconium hydrides. Also of interest is the puzzle why ZrH_3 has the same stoichiometry and similar structure as H_3S but does not have a T_c as nearly close to the latter. The H_3S under a pressure of 153 GPa shows both a Meissner effect and zero electrical resistivity with a high T_c of 203 K. To probe the relative superconductivity of ZrH_3 and H_3S, we compare their T_c's and associated parameters in Table 1. We note that the λ and $\omega_{\log}$ in ZrH_3 are significantly smaller than those for H_3S, which explains the fairly low T_c in ZrH_3. According to eq 1, the T_c is linearly proportional to $\omega_{\log}$. Numerically, $\omega_{\log}$ of H_3S is about twice that of ZrH_3, but the T_c of H_3S is 19−25 times greater than that of ZrH_3, indicating that the EPC strength λ dominates the estimated T_c (Table 1). As mentioned above, the electron−phonon interaction of hydrogen contributes 51% to the total λ in ZrH_3, much lower than that over 80% in H_3S. To further explore the electron−phonon coupling, we note that[45]

$$\lambda = \frac{N(\varepsilon_f)\langle I^2\rangle}{M\langle\omega^2\rangle}, \quad \langle\omega^2\rangle = \frac{2}{\lambda}\int \alpha^2F(\omega)\omega\,d\omega \tag{2}$$

where $\langle I^2\rangle$ is the average over the Fermi surface of the electron−phonon matrix element and M is the atomic mass. Given that M is a constant, we present the other three parameters in Table 1. As is shown, although ZrH_3 has a larger DOS at the Fermi level $N(\varepsilon_f)$ than H_3S, the H states contribute much less, which is not favorable to EPC. In addition, a larger mass for the metal element and smaller electron−phonon matrix element also result in a weaker λ of ZrH_3, giving a much lower T_c than that of H_3S.

In summary, a mixture phase of ZrH_3 and Zr_4H_{15} was obtained by direct reaction of Zr + H_2 at 47.0 GPa, and by reacting ZrH_2 + H_2 at 30.4 GPa. Upon increasing the pressure, the two phases persist to 93.4 GPa without any phase transition or decomposition. ZrH_3 and Zr_4H_{15} are isostructural to A15 and Th_4H_{15} structures, respectively. This is the first time that stoichiometry like ZrH_3 and Zr_4H_{15} is realized for group IVB hydrides. Theoretical prediction, electrical resistance, and external magnetic experiments reveal that both ZrH_3 and Zr_4H_{15} are conventional superconducting materials, with the measured superconducting transition temperatures of 6.4 and 4.0 K at 40 GPa, respectively. Our results provide a reference for the synthesis of new hydrogen-rich materials under high pressures and the exploration of metal hydrides. Polyhydrides of zirconium with higher hydrogen content may exist at even higher pressures suggesting the need for further experiments to explore these systems.

■ ASSOCIATED CONTENT

Supporting Information

The Supporting Information is available free of charge at https://pubs.acs.org/doi/10.1021/acs.jpclett.9b03632.

> Computational and experimental methods, phase stability and metastable structures, calculated phonon dispersion curves, formation enthalpies, electronic band structures and PDOS, electrical measurement for ZrH_2, experimental XRD pattern, and structural information (PDF)

■ AUTHOR INFORMATION

Corresponding Authors

Defang Duan − *Jilin University, Changchun, China, and University of Cambridge, Cambridge, United Kingdom;* orcid.org/0000-0002-6878-1830; Email: duandf@jlu.edu.cn

Xiaoli Huang − *Jilin University, Changchun, China;* orcid.org/0000-0001-9628-5618; Email: huangxiaoli@jlu.edu.cn

Tian Cui − *Jilin University, Changchun, China, and Ningbo University, Ningbo, China;* orcid.org/0000-0002-9664-848X; Email: cuitian@jlu.edu.cn

Other Authors

Hui Xie − *Jilin University, Changchun, China*

Wenting Zhang − *Jilin University, Changchun, China*

Yanping Huang − *Jilin University, Changchun, China*

Hao Song − *Jilin University, Changchun, China*

Xiaolei Feng − *Center for High Pressure Science and Technology Advanced Research (HPSTAR), Beijing, China, and University of Cambridge, Cambridge, United Kingdom*

Yansun Yao − *University of Saskatchewan, Saskatoon, Canada*

Chris J. Pickard − *University of Cambridge, Cambridge, United Kingdom, and Tohoku University, Sendai, Japan*

Complete contact information is available at: https://pubs.acs.org/10.1021/acs.jpclett.9b03632

Author Contributions

[#]H.X. and W.Z. contributed equally. D.D. and T.C. designed the research; H.X., D.D., and C.J.P. performed the theoretical calculations; W.Z., X.H., and Y.H. performed the experiments; H.X., D.D., X.H., Y.H., H.S., Y.Y., C.J.P., and T.C. analyzed the data; H.X., X.F., D.D., X.H., Y.Y., C.P., and T. C. wrote the Letter.

Notes

The authors declare no competing financial interest.

■ ACKNOWLEDGMENTS

This work was supported by the National Key R&D Program of China (No. 2018YFA0305900), National Natural Science Foundation of China (Nos. 51632002, 11674122, 51572108, and 11504127), Program for Changjiang Scholars and Innovative Research Team in University (No. IRT_15R23), the 111 Project (No. B12011), and the Natural Sciences and Engineering Research Council of Canada (NSERC). C.J.P. acknowledges financial support from the Engineering and Physical Sciences Research Council (Grant EP/P022596/1) and a Royal Society Wolfson Research Merit award. Parts of the calculations were performed in the High Performance Computing Center (HPCC) of Jilin University and TianHe-1(A) at the National Supercomputer Center in Tianjin.

■ REFERENCES

(1) Duan, D.; Liu, Y.; Ma, Y.; Shao, Z.; Liu, B.; Cui, T. Structure and superconductivity of hydrides at high pressures. *Natl. Sci. Rev.* **2016**, *4*, 121−135.

(2) Gor'kov, L. P.; Kresin, V. Z. Colloquium: High pressure and road to room temperature superconductivity. *Rev. Mod. Phys.* **2018**, *90*, 011001.

(3) Zurek, E.; Bi, T. High-temperature superconductivity in alkaline and rare earth polyhydrides at high pressure: A theoretical perspective. *J. Chem. Phys.* **2019**, *150*, 050901.

(4) Drozdov, A. P.; Eremets, M. I.; Troyan, I. A.; Ksenofontov, V.; Shylin, S. I. Conventional superconductivity at 203 K at high pressures in the sulfur hydride system. *Nature* **2015**, *525*, 73.

(5) Einaga, M.; Sakata, M.; Ishikawa, T.; Shimizu, K.; Eremets, M. I.; Drozdov, A. P.; Troyan, I. A.; Hirao, N.; Ohishi, Y. Crystal structure of the superconducting phase of sulfur hydride. *Nat. Phys.* **2016**, *12*, 835.

(6) Drozdov, A. P.; Kong, P. P.; Minkov, V. S.; Besedin, S. P.; Kuzovnikov, M. A.; Mozaffari, S.; Balicas, L.; Balakirev, F. F.; Graf, D. E.; Prakapenka, V. B.; et al. Superconductivity at 250 K in lanthanum hydride under high pressures. *Nature* **2019**, *569*, 528−531.

(7) Somayazulu, M.; Ahart, M.; Mishra, A. K.; Geballe, Z. M.; Baldini, M.; Meng, Y.; Struzhkin, V. V.; Hemley, R. J. Evidence for Superconductivity above 260 K in Lanthanum Superhydride at Megabar Pressures. *Phys. Rev. Lett.* **2019**, *122*, 027001.

(8) Duan, D.; Liu, Y.; Tian, F.; Li, D.; Huang, X.; Zhao, Z.; Yu, H.; Liu, B.; Tian, W.; Cui, T. Pressure-induced metallization of dense $(H_2S)_2H_2$ with high-Tc superconductivity. *Sci. Rep.* **2015**, *4*, 6968.

(9) Liu, H.; Naumov, I. I.; Hoffmann, R.; Ashcroft, N. W.; Hemley, R. J. Potential high-T_c superconducting lanthanum and yttrium hydrides at high pressure. *Proc. Natl. Acad. Sci. U. S. A.* **2017**, *114*, 6990−6995.

(10) Peng, F.; Sun, Y.; Pickard, C. J.; Needs, R. J.; Wu, Q.; Ma, Y. Hydrogen Clathrate Structures in Rare Earth Hydrides at High Pressures: Possible Route to Room-Temperature Superconductivity. *Phys. Rev. Lett.* **2017**, *119*, 107001.

(11) Pickard, C. J.; Needs, R. J. High-pressure phases of silane. *Phys. Rev. Lett.* **2006**, *97*, 045504.

(12) Pickard, C. J.; Needs, R. J. Metallization of aluminum hydride at high pressures: A first-principles study. *Phys. Rev. B: Condens. Matter Mater. Phys.* **2007**, *76*, 144114.

(13) Eremets, M. I.; Trojan, I. A.; Medvedev, S. A.; Tse, J. S.; Yao, Y. Superconductivity in Hydrogen Dominant Materials: Silane. *Science* **2008**, *319*, 1506.

(14) Goncharenko, I.; Eremets, M. I.; Hanfland, M.; Tse, J. S.; Amboage, M.; Yao, Y.; Trojan, I. A. Pressure-induced hydrogen-dominant metallic state in aluminum hydride. *Phys. Rev. Lett.* **2008**, *100*, 045504.

(15) Rousseau, B.; Bergara, A. Giant anharmonicity suppresses superconductivity in AlH_3 under pressure. *Phys. Rev. B: Condens. Matter Mater. Phys.* **2010**, *82*, 104504.

(16) Shamp, A.; Zurek, E. Superconducting High-Pressure Phases Composed of Hydrogen and Iodine. *J. Phys. Chem. Lett.* **2015**, *6*, 4067−4072.

(17) Shamp, A.; Terpstra, T.; Bi, T.; Falls, Z.; Avery, P.; Zurek, E. Decomposition Products of Phosphine Under Pressure: PH2 Stable and Superconducting? *J. Am. Chem. Soc.* **2016**, *138*, 1884−1892.

(18) Wang, L.; Duan, D.; Yu, H.; Xie, H.; Huang, X.; Ma, Y.; Tian, F.; Li, D.; Liu, B.; Cui, T. High-Pressure Formation of Cobalt Polyhydrides: A First-Principle Study. *Inorg. Chem.* **2018**, *57*, 181−186.

(19) Gao, G.; Wang, H.; Zhu, L.; Ma, Y. Pressure-Induced Formation of Noble Metal Hydrides. *J. Phys. Chem. C* **2012**, *116*, 1995−2000.

(20) Kvashnin, A. G.; Semenok, D. V.; Kruglov, I. A.; Wrona, I. A.; Oganov, A. R. High-Temperature Superconductivity in a Th−H System under Pressure Conditions. *ACS Appl. Mater. Interfaces* **2018**, *10*, 43809−43816.

(21) Semenok, D. V.; Kvashnin, A. G.; Kruglov, I. A.; Oganov, A. R. Actinium Hydrides AcH_{10}, AcH_{12}, and AcH_{16} as High-Temperature Conventional Superconductors. *J. Phys. Chem. Lett.* **2018**, *9*, 1920−1926.

(22) Li, B.; Ding, Y.; Kim, D. Y.; Ahuja, R.; Zou, G.; Mao, H. K. Rhodium dihydride (RhH_2) with high volumetric hydrogen density. *Proc. Natl. Acad. Sci. U. S. A.* **2011**, *108*, 18618−21.

(23) Wang, M.; Binns, J.; Donnelly, M.-E.; Peña-Alvarez, M.; Dalladay-Simpson, P.; Howie, R. T. High pressure synthesis and stability of cobalt hydrides. *J. Chem. Phys.* **2018**, *148*, 144310.

(24) Pépin, C. M.; Geneste, G.; Dewaele, A.; Mezouar, M.; Loubeyre, P. Synthesis of FeH_5: A layered structure with atomic hydrogen slabs. *Science* **2017**, *357*, 382.

(25) Liu, C.; Jiang, S.; Sui, Y.; Chen, Y.; Xiao, G.; Chen, X.-J.; Shu, H.; Duan, D.; Li, X.; Liu, H.; et al. Effect of the Inherent Structure of Rh Nanocrystals on the Hydriding Behavior under Pressure. *J. Phys. Chem. Lett.* **2019**, *10*, 774−779.

(26) Singh, R. N.; Bind, A. K.; Srinivasan, N. S.; StÅhle, P. Influence of hydrogen content on fracture toughness of CWSR Zr−2.5Nb pressure tube alloy. *J. Nucl. Mater.* **2013**, *432*, 87−93.

(27) Zuzek, E.; Abriata, J. P.; San-Martin, A.; Manchester, F. D. The H-Zr (hydrogen-zirconium) system. *Bull. Alloy Phase Diagrams* **1990**, *11*, 385−395.

(28) Root, J. H.; Small, W. M.; Khatamian, D.; Woo, O. T. Kinetics of the δ to γ zirconium hydride transformation in Zr-2.5Nb. *Acta Mater.* **2003**, *51*, 2041−2053.

(29) Li, X. F.; Hu, Z. Y.; Huang, B. Phase diagram and superconductivity of compressed zirconium hydrides. *Phys. Chem. Chem. Phys.* **2017**, *19*, 3538−3543.

(30) Abe, K. High-pressure properties of dense metallic zirconium hydrides studied by ab initio calculations. *Phys. Rev. B: Condens. Matter Mater. Phys.* **2018**, *98*, 134103.

(31) Wang, Y.; Lv, J.; Zhu, L.; Ma, Y. Crystal structure prediction via particle-swarm optimization. *Phys. Rev. B: Condens. Matter Mater. Phys.* **2010**, *82*, 094116.

(32) Pickard, C. J.; Needs, R. J. Ab initiorandom structure searching. *J. Phys.: Condens. Matter* **2011**, *23*, 053201.

(33) Zachariasen, W. Crystal chemical studies of the 5f-series of elements. XIX. The crystal structure of the higher thorium hydride, Th_4H_{15}. *Acta Crystallogr.* **1953**, *6*, 393−395.

(34) Loubeyre, P.; LeToullec, R.; Hausermann, D.; Hanfland, M.; Hemley, R. J.; Mao, H. K.; Finger, L. W. X-ray diffraction and equation of state of hydrogen at megabar pressures. *Nature* **1996**, *383*, 702−704.

(35) Stavrou, E.; Yang, L. H.; Söderlind, P.; Aberg, D.; Radousky, H. B.; Armstrong, M. R.; Belof, J. L.; Kunz, M.; Greenberg, E.; Prakapenka, V. B.; et al. Anharmonicity-induced first-order isostructural phase transition of zirconium under pressure. *Phys. Rev. B: Condens. Matter Mater. Phys.* **2018**, *98*, 220101.

(36) Birch, F. The Effect of Pressure Upon the Elastic Parameters of Isotropic Solids, According to Murnaghan's Theory of Finite Strain. *J. Appl. Phys.* **1938**, *9*, 279−288.

(37) Sidhu, S. S.; McGuire, J. C. An X-Ray Diffraction Study of the Hafnium-Hydrogen System. *J. Appl. Phys.* **1952**, *23*, 1257−1261.

(38) Sidhu, S. S. The effect on metal−metal bonds of increased concentration of hydrogen in hafnium dihydride. *Acta Crystallogr.* **1954**, *7*, 447−449.

(39) Kalita, P. E.; Sinogeikin, S. V.; Lipinska-Kalita, K.; Hartmann, T.; Ke, X.; Chen, C.; Cornelius, A. Equation of state of TiH_2 up to 90 GPa: A synchrotron x-ray diffraction study and ab initio calculations. *J. Appl. Phys.* **2010**, *108*, 043511.

(40) Allen, P. B.; Dynes, R. C. Transition temperature of strong-coupled superconductors reanalyzed. *Phys. Rev. B* **1975**, *12*, 905−922.

(41) Woollam, J. A.; Somoano, R. B.; O'Connor, P. Positive Curvature of the H_{c2}-versus-T_c Boundaries in Layered Superconductors. *Phys. Rev. Lett.* **1974**, *32*, 712−714.

(42) Baumgartner, T.; Eisterer, M.; Weber, H. W.; Flükiger, R.; Scheuerlein, C.; Bottura, L. Effects of neutron irradiation on pinning force scaling in state-of-the-art Nb_3Sn wires. *Supercond. Sci. Technol.* **2014**, *27*, 015005.

(43) Errea, I.; Calandra, M.; Pickard, C. J.; Nelson, J.; Needs, R. J.; Li, Y.; Liu, H.; Zhang, Y.; Ma, Y.; Mauri, F. High-Pressure Hydrogen Sulfide from First Principles: A Strongly Anharmonic Phonon-Mediated Superconductor. *Phys. Rev. Lett.* **2015**, *114*, 157004.

(44) Richardson, C. F.; Ashcroft, N. W. High Temperature Superconductivity in Metallic Hydrogen: Electron-Electron Enhancements. *Phys. Rev. Lett.* **1997**, *78*, 118−121.

(45) McMillan, W. L. Transition Temperature of Strong-Coupled Superconductors. *Phys. Rev.* **1968**, *167*, 331−344.